Software Defined Radio Demonstration of MIMO-OFDM Rate Adaptation

John Kountouriotis, Nicholas J. Kirsch, and Kapil R. Dandekar
Department of Electrical and Computer Engineering
Drexel University
Philadelphia, PA 19104
Email: {jk368, njk27, dandekar}@drexel.edu

***Abstract*— In this paper, we present a framework for rate and power allocation in MIMO-OFDM systems using the V-BLAST and SVD techniques. The performance of these techniques are compared with one another and with waterfilling using channel measurements on our MIMO-OFDM software defined radio testbed. Specifically, we show with measured data that sub-carrier rate adaptation allows for more efficient spectral use. Furthermore, we show that power allocation over streams provides significant gains as well. We analyze the impact of stale channel feedback information on this rate and power allocation framework and demonstrate how matrix channel prediction using a Kalman-filter based, vector autoregressive model can alleviate this problem.**

I. Introduction

Software Defined Radio (SDR) technology makes use of highly flexible radios that are able to use multiple communication standards on the same hardware [1]. This technology is extremely valuable to the research community, since an SDR platform can be used for experiments on multiple communication schemes inexpensively compared to traditional approaches.

Over the past few years, the data rate of wireless communications has increased due to new techniques in signal processing and spatial diversity. Multiple-input multiple-output (MIMO) systems have the benefit of linearly increasing data rate with an increase in antenna array size. Orthogonal frequency division multiplexing (OFDM) can provide higher data rates over a frequency selective channel by transmitting data on multiple narrowband carriers. With the advent of SDR, wireless communications has taken a step forward in the ability to implement flexible algorithms to dynamically adapt to the state of the propagation channel.

Various SDR architectures of MIMO [2], [3] or MIMO-OFDM [4], [6], [7] communication systems have been implemented ([5] and references therein). The authors of [2] built a MIMO SDR experimental platform to explore Low-Density Parity-Check (LDPC) codes. This two node 4×4 system (links with 4 transmit and 4 receive antennas) allows for configuring and testing of new coding schemes. Similarly, another SDR platform has been designed to consider different spatial multiplexing schemes [3]. This 2×2 system is implemented in DSP boards to allow for real-time demonstration of the performance of different coding schemes. A non real-time DSP-based SDR platform aimed at implementing physical layer algorithms [5] has been used to analyze the performance of space-time trellis coding. Outdoor performance of a MIMO-OFDM SDR system can be found in [6].

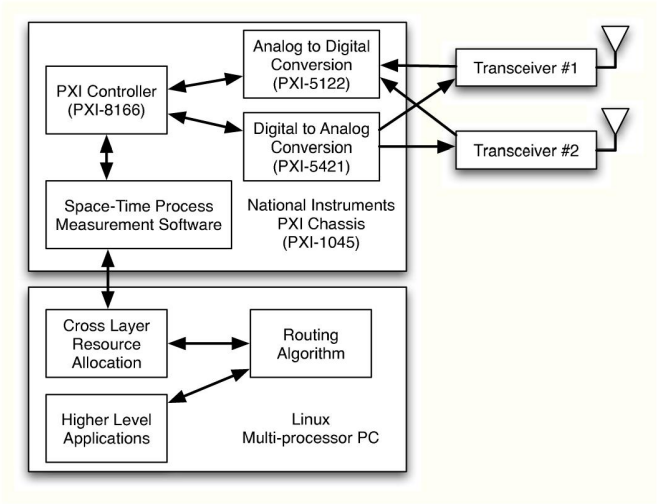

Fig. 1. Software Defined Radio Testbed Block Diagram

Out testbed [4], [7] allows for definition of not only coding schemes but also supports OFDM. This five node 2×2 antenna MIMO-OFDM system, allows for the testing of larger networks of MIMO links. The system is designed for maximum flexibility in cross layer algorithms at the expense of slower than real-time operation. A block diagram of our system is shown in Fig. 1. A picture of a network node can be seen in Fig. 2.

The goal of this paper is to provide a framework for rate and power adaptation in a MIMO-OFDM system through experimental measurements on an SDR platform. Previous work has explored adaptive techniques for modulation over each OFDM sub-carrier [8]–[10]. Sub-carrier rate adaption allows for more efficient spectral use by tuning the rates of each sub-carrier based upon estimated channel conditions. This prior work [8] either assumed that power is fixed over each sub-carrier, or assumed a fixed rate [9], [10].

We propose a technique to optimize not only rate, but also power, over sub-carriers to better utilize available spectral

1-4244-0733-8/06/$20.00 ©2006 IEEE

Fig. 2. MIMO-OFDM SDR node

resources based on channel conditions. We also quantify the impact of stale estimates of channel state information (CSI) on our algorithm and demonstrate how a Kalman-filter based, vector autoregressive model can alleviate bit error rate (BER) performance degradation. All techniques described in the paper were evaluated using measured channels from our MIMO-OFDM SDR testbed, described more in detail at section IV.

II. System Model

We consider a broadband MIMO system employing M_t transmit and M_r receive antennas. The symbol vector $\mathbf{x}(n)$ is transmitted through a complex-valued random MIMO fading channel, $\mathbf{H}_l$, of size $M_r \times M_t$. $\mathbf{H}_l$ represents the l^{th} delayed time tap of the discrete-time MIMO channel impulse response, and L is the total number of time taps. The matrix-valued transfer function [11] is,

$$\mathbf{H}(e^{j2\pi\theta}) = \sum_{l=0}^{L-1} \mathbf{H}_l e^{-j2\pi l\theta} \tag{1}$$

where θ is a random variable with $0 \leq \theta < 1$.

The main motivation for using OFDM, is to transform the frequency-selective MIMO channel into a set of parallel frequency-flat MIMO channels. More specifically, the symbols to be transmitted are organized into frequency vectors of length N, where N denotes the number of sub-carriers or tones, our system is using. If we assume a correct choice of cyclic prefix (CP) and perfect synchronization for sampling so that the interference from adjacent sub-carriers is completely removed [12], the input-output relationship of the system on a tone by tone basis is,

$$\mathbf{y}_k = \mathbf{H}_k \mathbf{x}_k + \mathbf{n}_k \tag{2}$$

for the k^{th} sub-carrier. $\mathbf{y}_k$ is the $M_r \times 1$ received signal vector, $\mathbf{H}_k$ is the $M_r \times M_t$ channel matrix, $\mathbf{x}_k$ is the $M_t \times 1$ transmitted signal vector, and $\mathbf{n}_k$ is the complex-valued, circularly symmetric additive white Gaussian noise vector.

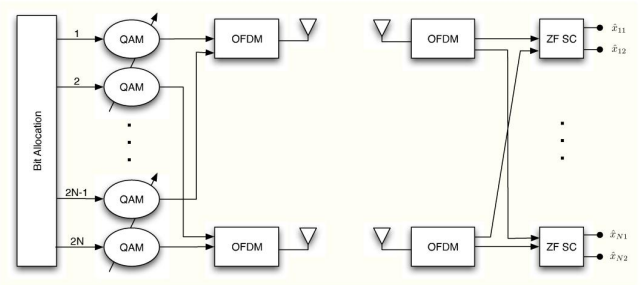

Fig. 3. V-BLAST for a 2×2 MIMO-OFDM system with N sub-carriers

Certain MIMO channel conditions lead to the situation where the channel gains are uncorrelated. This occurs for high rank $\mathbf{H}_k$ matrices. When this condition occurs, there are multiple "streams", that can be used for communications. In this paper, we refer to the j^{th} particular stream of J_k total streams, where J_k is the number of non-zero singular values of $\mathbf{H}_k$. In the rest of the document, unless otherwise specified, the equations written involving $\mathbf{y}$, $\mathbf{H}$, $\mathbf{x}$, J, and $\mathbf{n}$ will refer to the sub-carrier quantity without specifying the subscript k.

III. MIMO Transmission Techniques and Rate Adaptation

We continue our discussion by implementing different rate adaptation techniques in software in order to adapt the communications system efficiently in the presence of changing channel effects.

A. V-BLAST with Zero Forcing and Limited Channel Feedback

The V-BLAST (Vertical Bell Laboratories Layered Space Time) architecture was developed by Foschini, *et. al.* [13], [14]. As shown in Fig. 3, the data bits to be transmitted are demultiplexed into M_t parallel streams per sub-carrier (though not all sub-carriers may be used) and are mapped from bit-to-symbol, where all M_t symbols per sub-carrier are drawn from the same constellation. The symbols are passed through an OFDM modulator and then transmitted in parallel from the M_t antennas [13], [14]. Unlike the SVD method, discussed later in this paper, V-BLAST does not require any inter-stream coding. The transmit power of each antenna and sub-carrier is fixed.

The post-processing SNR of the j^{th} stream is

$$\text{SNR}_j = \frac{|\mathbf{x}_j|^2}{N_0 |\mathbf{w}_j|^2} \tag{3}$$

where N_0 is defined such that $E\{nn^H\} = N_0 \mathbf{I}_{\mathbf{M_r}}$, $E\{\cdot\}$ denotes expectation and $\mathbf{I}_{\mathbf{M_r}}$ is an identity matrix for size $M_r \times M_r$. $\mathbf{w}_j$ is the minimum norm row of the pseudoinverse of the channel matrix $\mathbf{H}$.

The non-linear procedure of ordering the estimation and successive cancellation guarantees that the SNR over all streams is maximized [13], [14]. Also, as a consequence of the Cauchy-Schwartz inequality, the overall SNR is lower bounded

by the SNR of the first detected stream [13], [14]. The lower bound on SNR possible with V-BLAST will also provide a upper bound for BER. However, this BER bound will only hold when the same constellation is used for all the streams in the transmitted vector.

When different modulation constellations are used, the BER is no longer a function of only the SNR, but also of the constellation in use. In general, as the constellation size grows, the BER performance for a given SNR level decreases. Thus, if different constellations are used on different streams of the same sub-carrier, the Zero Forcing (ZF) algorithm with Successive Cancellation (SC) procedure might yield worst BER performance than if no particularly ordering was used for cancellation, as shown in [15].

The goal in rate adaptation is to adjust the modulation index of the signal constellation given feedback from the receiver, to meet the SNR requirements for successful communication. This feedback can either be performed by using one constellation on all sub-carriers and streams, which is equivalent to setting the constellation size by the worst SNR sub-carrier. This flavor of VBLAST will be referred as VBLAST1 for performance evaluation purposes. Alternatively, feedback can be performed on a sub-carrier by sub-carrier basis. In the latter case, the streams in each sub-carrier will use the same constellation, however this constellation will vary from sub-carrier to sub-carrier. This second variant of VBLAST will be referred to as VBLAST2.

B. SVD Method and Full Channel Feedback

In the case where full CSI (channel state information) is available at the transmitter, the SVD method [16] is an alternative to the V-BLAST method. In the SVD method, each antenna transmits a linear combination of all streams, as opposed to V-BLAST, where each stream is transmitted by one antenna. The MIMO-OFDM matrix channel at each sub-carrier can be decomposed using singular value decomposition as $\mathbf{H} = \mathbf{USV}^*$, where * denotes the complex conjugate transpose.

As shown in Fig. 4, the data bits to be transmitted are demultiplexed into M_t parallel streams per sub-carrier (though not all streams in every sub-carrier may be used) and are mapped independently from bit-to-symbol (to symbol vector $\mathbf{x}$) from potentially different signal constellations. The transmitted symbol vector per sub-carrier, $\dot{\mathbf{x}}$, is the symbol vector per sub-carrier $\mathbf{x}$ pre-multiplied by matrix $\mathbf{V}$ [16]. The input to the OFDM modulator for a particular sub-carrier is a linear combination of all streams in that sub-carrier.

The received signal vector, per sub-carrier, is $\mathbf{y} = \mathbf{USx}+\mathbf{n}$. This received vector is post-multiplied by $\mathbf{U}^*$. We see that the above procedure decouples the $M_t \times M_r$ MIMO channel into J parallel single input single output (SISO) streams, where J equals the number of non-zero singular values of $\mathbf{H}$, $1 \leq j \leq \min(M_r, M_t)$. The post processing SNR of stream j, in terms of the j^{th} singular value λ_j of $\mathbf{H}$ is

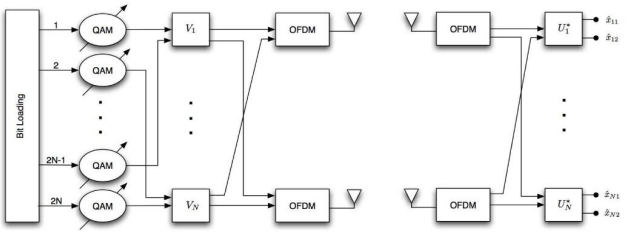

Fig. 4. SVD for a 2×2 MIMO-OFDM system with N sub-carriers

$$\text{SNR}_j = \frac{\lambda_j^2 |\mathbf{x}_j|^2}{N_0}. \tag{4}$$

The power allocation that maximizes the theoretical capacity of the above scheme is given by the well known waterfilling solution [16], where the power is allocated per stream and sub-carrier as,

$$p_j^{(k)} = \left(\mu - \frac{1}{(\lambda_j^{(k)})^2} \right)^+ \tag{5}$$

where $p_j^{(k)}$ is the power allocated to the j^{th} stream of the k^{th} sub-carrier and μ is the "water level" specified by the total available transmit power P_T, using $\sum_{k=1}^{N} \sum_{j=1}^{J} p_j^{(k)} = P_T$. J is the number of non-zero singular values of the channel matrix of the k_{th} sub-carrier.

This maximization scheme does not take into account the fact that in practice we have to use constellations that consist of an integer number of bits, b, usually $b \in \{1, \ldots, 6\}$ (i.e. BPSK to 64-QAM). In this practical situation, waterfilling, while maximizing the theoretical capacity, does not maximize the total number of bits that a single MIMO-OFDM symbol can carry. This non-optimal loading occurs, first, because the technique may assign power to streams that are too weak to carry at least 1 bit (thus this power is never really "assigned"). Secondly, the technique may assign more power than necessary to transmit an integer number of bits.

The wasted power from these "bit quantization" errors, if gathered from all streams and sub-carriers, can be efficiently re-assigned to a smaller number of streams than the original power allocation so that more bits can be carried per symbol. This reduction in the number of streams can be done in the same way as described in [17], [18], where the authors investigate the problem of assigning power in a SISO-OFDM system. The difference in our situation [17], [18] is that we possibly have more than one symbol stream per sub-carrier.

To address this bit loading issue, a table is constructed with the values of power that need to be assigned to each stream in order to carry an additional bit, given some BER constraint [17]. Since we start with no bits being allocated, the initial values are the power that need to be assigned so that the stream will be able to carry one bit. Until all of the available power is allocated, in each step, we choose the minimum value from the

table. Next, we assign the respective stream one bit and deduct the power required for this allocation from the total available power. We then update the table value for that particular stream to reflect the power required to add an additional bit and repeat the procedure until all power is allocated. While the above procedure is not waterfilling in the classical sense, quoting the words from [17] "since it puts every increment of power where it will be more effective, it appears to be optimum for multicarrier transmission using QAM constellations and symbol by symbol detection".

We investigate two different versions of the SVD method. In the first version, SVD1, we keep the power per sub-carrier constant and perform the above bit loading algorithm per sub-carrier (between the two streams of the sub-carrier). In the second version, SVD2, the bit loading algorithm is performed along all of the sub-carriers. In SVD2, after the completion of the algorithm, the power assigned per sub-carrier is different.

IV. Measurement Configuration

For our measurements the Drexel University Wireless System Laboratory in collaboration with the Wireless Networking & Communications Group at the University of Texas at Austin developed a custom software defined multiple antenna mobile ad hoc network. Each node in our experimental platform consists of frequency agile transceivers in the ISM and UNII radio operating bands and a baseband process computer. The baseband chassis provided by National Instruments has two major functional roles. First, the unit runs the analog to digital (A/D) and (D/A) converters required to for two transceivers. The converters operate at 100 MS/s with 14-bit quantization. Second, the baseband unit is a software defined radio (SDR). This allows for the unique ability to tailor the communication scheme for a given experiment. An overview of the testbed can be seen in Figure 1.

To test our optimization, we collected channel measurements for a 2×2 MIMO SDR communication system. The spacing of the antennas was one wavelength operating at 2.484 GHz. The measurements were made in an indoor environment on the 3rd floor of the Bossone building on the campus of Drexel University. The 20 MHz system bandwidth is separated into 64, 31.25 kHz OFDM sub-carriers. The system deployed is similar to the 802.11a scheme which only uses 52 sub-carriers. In each measurement, 100 snapshots of the MIMO channel are recorded. Our measured channels are then used to analyze the different rate adaptation schemes.

V. Results

Table I is provided to aid the reader in comparing and contrasting the techniques used in this paper. Our analysis will consider BPSK and QAM modulation (with modulation index from $M \in \{4, \ldots, 64\}$) and a BER of 10^{-3}. The calculation of the BER as a function of SNR is [19],

$$P_b \approx 0.2 \exp\left(\frac{-gE_s}{No}\right), \tag{6}$$

Waterfilling1	Power per sub-carrier fixed
Waterfilling2	Power varies across sub-carriers
V-BLAST1	Symbols use the same constellation (integer bit load)
V-BLAST2	Symbol constellation varies over sub-carrier (int. bit load)
SVD1	Power per sub-carrier fixed (integer bit load)
SVD2	Power varies across sub-carriers (integer bit load)

TABLE I
ABBREVIATION REFERENCE FOR ALLOCATION TECHNIQUES

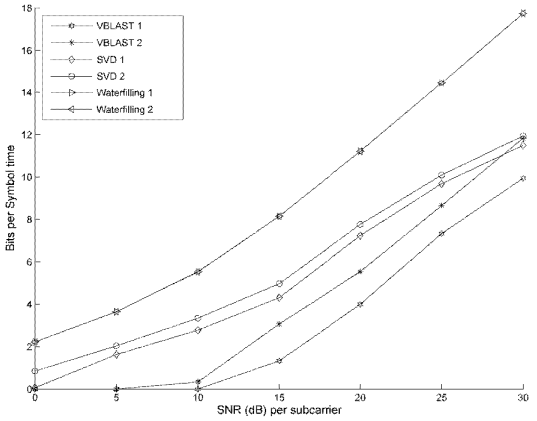

Fig. 5. Capacity for the methods

where $g = \frac{3}{2(M-1)}$ for square QAM (M=4, 16 and 64) and $g = \frac{6}{5M-4}$ for rectangular QAM (M=8 and 32). The BPSK case is a special case of rectangular QAM and is treated with the corresponding formula for M=2 [19].

A. Known Channel Information

Fig. 5 shows the capacity, measured in bits per symbol time, based upon the measured channel using both the V-BLAST and SVD methods for various SNR values. Along with these methods, the theoretical capacity obtained using the waterfilling procedure is also used as a benchmark. The waterfilling method is used assuming infinite granularity in our constellation size, opposed to an integer constellation size for V-BLAST and SVD methods. Waterfilling1 is analogous to SVD1 and Waterfilling2 is analogous to SVD2.

The capacity for Waterfilling1 coincides with Waterfilling2. From this overlap, we conclude that allocating the total available power in a per sub-carrier basis does not matter. However, if we compare the performance of SVD1 and SVD2, the integer bit constraint we are imposing on our system limits the achievable capacity. Furthermore, SVD2 capacity is greater than SVD1 capacity due to the additional degree of freedom in allocating power over both sub-carrier and stream. When power is allocated per sub-carrier, excess power may remain when an additional bit cannot be loaded. The results from SVD2 compared with SVD1 show that If we have the

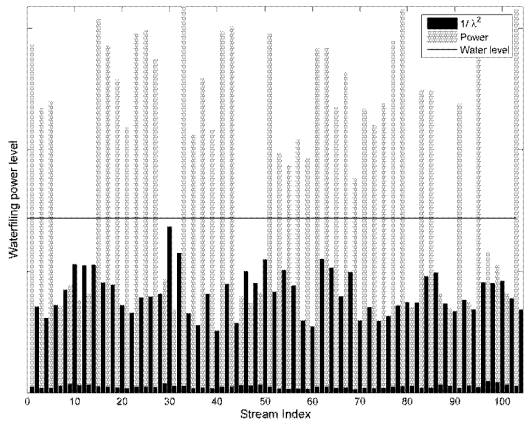

Fig. 6. Power allocated by SVD2 per stream at an of SNR 15 dB

flexibility to gather excess power from all the sub-carriers, this power may be enough to load additional bits.

As expected, the two V-BLAST methods perform worse than the SVD methods. This result occurs because the V-BLAST techniques use an "all or nothing" strategy (i.e. two streams are used per sub-carrier or none). The capacity at a given SNR is higher for V-BLAST2 in comparison with V-BLAST1. This is because V-BLAST1 transmits nothing unless all of the sub-carriers can be loaded with two streams compared to V-BLAST2 which does not transmit only when the two streams for one sub-carrier cannot be loaded.

Both SVD methods reduce to a beamforming scheme at low SNRs, where only one of the available streams is loaded with a symbol. When the difference in the singular values per sub-carrier is relatively large (and both streams are used in a sub-carrier at high SNRs > 15 dB), symbols are assigned from different constellations in the two streams of a sub-carrier. For example, when the SNR is very high, both the streams will be loaded with a symbol from the 64-QAM constellation.

In Fig. 6, we show the waterfilling graph for a given snapshot of our channel measurements at an SNR level of 15 dB per sub-carrier. The power that is assigned for the SVD2 case is stacked on top of the $1/\lambda_j^2$ computed for waterfilling calculations. The line shown is the "water level" as calculated using the classical waterfilling method in Eq. 5. Since the "water level" is above all of the $1/\lambda_j^2$ values, the classical waterfilling solution has assigned power to all streams (with the power per stream given by the difference between the "water level" and $1/\lambda_j^2$) . We see that some streams in the SVD2 power allocation have been assigned a lot more power than the water filling solution would allow, whereas some other streams do have any power allocated to them. This difference in power allocation occurs due to the integer bit constraint that we have imposed in the system.

B. Stale Channel Information

In the previous discussion of results, we have assumed that channel information is timely fed back to the transmitter in order to perform the discussed adaptation. In this section, we discuss the impact of stale channel knowledge on the discussed methods. The channel is described as "stale" because the channel used for adaptation represents an old estimate that may not adequately describe current conditions.

In the case of the SVD method, stale channel information leads to the wrong estimation of the singular vectors $\mathbf{U}$ and $\mathbf{V}$ that are used to diagonalize the channel matrix. In this case, the two streams on a given sub-carrier are no longer decoupled. Thus inter-stream "interference" is present [20], for the case where both of the streams will be loaded with bits (i.e. high SNR). Secondly, the channel gains are no longer representative of the channel, which leads us to load the bits across the sub-carriers in a suboptimal fashion.

In the case of the VBLAST methods, we still assume that the receiver has perfect channel knowledge so the correct pseudo-inverse channel matrix can be calculated. However the channel fed back to the transmitted may be stale. Thus, the transmitter with this stale channel knowledge, may load bits sub-optimally across the sub-carriers.

In order to limit the impact of stale channel information on the system, we use a matrix channel prediction algorithm, adopted from the vector channel prediction algorithm presented in [21]. The method uses a Kalman-filter based, vector autoregressive (VAR) model, in order to estimate the matrix channel based upon past knowledge. Channel estimates are used to train the system during a given training period. The Kalman filter approach reduces the computational complexity of the VAR model update during the training period. At the end of the training period, predictions are made using the VAR model for a certain prediction horizon [21].

In Fig. 7, the BER performance of the SVD techniques is presented with and without prediction. We can see that the prediction method performs very well in terms of BER for SNR lower than 12 dB, while for higher SNR, the BER becomes significant with and without prediction. In the high SNR region, both streams on each sub-carrier become active, which causes spatial interference and performance degradation. This spatial interference is because the channel matrix is not diagonalized by $\mathbf{U}$ and $\mathbf{V}$. In the SNR region above 25 dB, all the streams are fully loaded with data bits, which is why the BER curve stops increasing with increasing SNR.

To support this loading result, we refer to Fig. 8. In this graph, the number of streams per sub-carrier is shown for SVD1, SVD2 and VBLAST2 techniques. For the SVD methods, we see that the stronger stream in each sub-carrier gradually becomes active until SNR reaches 15 dB. For SNR above 15 dB, the second stream in each sub-carrier becomes active, and thus introduces inter stream interference. In the same graph, we see that the VBLAST2 method, gradually activates sub-carriers in the SNR region from 10 to 15 dB. For SNR greater than 15 dB, all sub-carriers and streams are

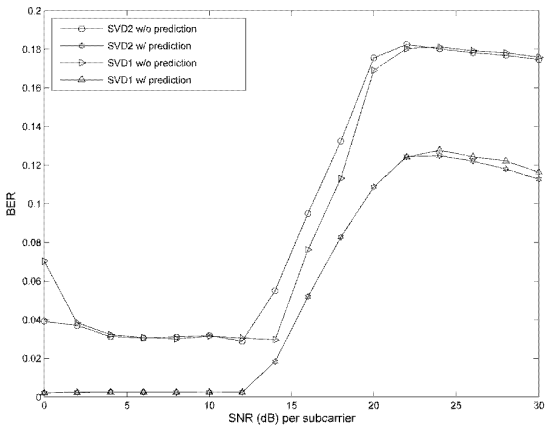

Fig. 7. Bit error rate comparison of the SVD techniques with and without prediction.

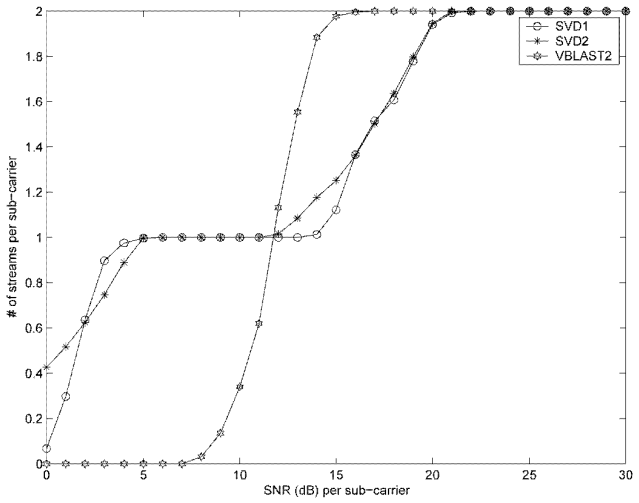

Fig. 8. Number of streams per sub-carrier as a function of SNR for SVD1, SVD2 and VBLAST2.

active for VBLAST2. We did not include in the same graph VBLAST1, since this technique simultaneously activates all sub-carriers, with two streams each, at an SNR of approximately 15 dB. Comparison of Fig. 8 and Fig. 7 shows that the BER follows the same pattern with increasing SNR as the number of streams per sub-carrier. However, when matrix channel prediction is used, the BER is insignificant in the low SNR region where the SVD methods are reduced to beamforming.

VI. Conclusions

In this paper, we have presented a framework for rate and power allocation in MIMO-OFDM systems using the V-BLAST and SVD techniques. The performance of these techniques were compared with one another and with waterfiling based upon channel measurements that were taken on our MIMO-OFDM software defined radio testbed. Specifically, we have shown with measured data that sub-carrier rate adaptation allows for more efficient spectral use. Furthermore, we show that control of power allocation over stream provides significant gains. Finally, we analyzed the impact of stale channel information on this power and rate adaptation framework and demonstrated how matrix channel prediction can suppress this problem. This research motivates the investigation of stronger channel estimation and prediction techniques. Also, work could be done to modify the V-BLAST technique to allow for single antenna transmission at low values of SNR.

Acknowledgment

This research is supported by the National Science Foundation under Grants 0435041 and 0322795. National Instruments has provided equipment donations supporting this research.

References

[1] J. Mitola, "Software radio architecture," *IEEE Communications Magazine*, vol. 33, no. 5, pp. 26 – 38, 1995.

[2] N. Chiurtu, L. Gasser, P. Roud, and B. Rimoldi, "Software-defined radio implementation of multiple antenna systems using low-density parity-check codes," *IEEE Wireless Communications and Networking Conference, WCNC*, vol. 1, pp. 527 – 531, 2005.

[3] R. Mostafa, R. Gozali, R. Palat, M. Robert, W. Newhall, B. Woerner, and J. Reed, "Design and implementation of a DSP-based MIMO system prototype for real-time demonstration and indoor channel measurements," *EURASIP Journal on Applied Signal Processing*, vol. 2005, no. 16, pp. 2673 – 85, 1 Sept. 2005.

[4] A. Gupta, A. Forenza, and R. W. Heath Jr., "Rapid MIMO-OFDM software defined radio system prototyping," *IEEE Workshop on Signal Processing Systems, SiPS: Design and Implementation*, pp. 182 – 187, 2004.

[5] R. M. Rao, W. Zhu, S. Lang, C. Oberli, D. Browne, J. Bhatia, J.-F. Frigon, J. Wang, P. Gupta, H. Lee, D. N. Liu, S. G. Wong, M. Fitz, B. Daneshrad, and O. Takeshita, "Multi-antenna testbeds for research and education in wireless communications," *IEEE Communications Magazine*, vol. 42, no. 12, pp. 72 – 81, 2004.

[6] H. Sampath, S. Talwar, J. Tellado, V. Erceg, and A. Paulraj, "A fourth-generation mimo-ofdm broadband wireless system: Design, performance, and field trial results," *IEEE Communications Magazine*, vol. 40, no. 9, pp. 143 – 149, 2002.

[7] D. Piazza and K. Dandekar, "Reconfigurable antenna solution for MIMO-OFDM systems," *Accepted for publication in IEE Electronics Letters*, 2006.

[8] T. Keller and L. Hanzo, "Adaptive multicarrier modulation: a convenient framework for time-frequency processing in wireless communications," *Proceedings of the IEEE*, vol. 88, pp. 611 – 640, 2000.

[9] J. H. Sung and J. R. Barry, "Rate-allocation strategies for closed-loop MIMO-OFDM," *IEEE Vehicular Technology Conference*, vol. 58, no. 1, pp. 483 – 487, 2004.

[10] ——, "Bit-allocation strategies for MIMO fading channels with channel knowledge at transmitter," *IEEE Vehicular Technology Conference*, vol. 57, no. 2, pp. 813 – 817, 2003.

[11] H. Bolcskei and A. Paulraj, "Space-frequency codes for broadband fading channels," *IEEE International Symposium on Information Theory - Proceedings*, pp. 219 – 224, 2001.

[12] H. Bölcskei, *Principles of MIMO-OFDM wireless systems*, 2004. [Online]. Available: http://www.nari.ee.ethz.ch/commth/pubs/p/crc03

[13] P. Wolniansky, G. Foschini, G. Golden, and R. Valenzuela, "V-BLAST: an architecture for realizing very high data rates over the rich-scattering wireless channel," *1998 URSI International Symposium on Signals, Systems, and Electronics*, pp. 295 – 300, 1998.

[14] G. Golden, C. Foschini, R. Valenzuela, and P. Wolniansky, "Detection algorithm and initial laboratory results using V-BLAST space-time communication architecture," *Electronics Letters*, vol. 35, no. 1, pp. 14 – 16, 1999.

[15] S. T. Chung, A. Lozano, H. C. Huang, A. Sutivong, and J. M. Cioffi, "Approaching the mimo capacity with a low-rate feedback channel in V-BLAST," *Eurasip Journal on Applied Signal Processing*, vol. 2004, no. 5, pp. 762 – 771, 2004.

[16] G. Raleigh and J. Cioffi, "Spatio-temporal coding for wireless communications," *Conference Record / IEEE Global Telecommunications Conference*, vol. 3, pp. 1809 – 1814, 1996.

[17] J. Bingham, "Multicarrier modulation for data transmission: an idea whose time has come," *IEEE Communications Magazine*, vol. 28, no. 5, pp. 5 – 14, 1990.

[18] P. S. Chow, J. M. Cioffi, and J. A. Bingham, "Practical discrete multitone transceiver loading algorithm for data transmission over spectrally shaped channels," *IEEE Transactions on Communications*, vol. 43, no. 2-4, pp. 773 – 775, 1995.

[19] S. Zhou and G. B. Giannakis, "Adaptive modulation for multiantenna transmissions with channel mean feedback," *IEEE Transactions on Wireless Communications*, vol. 3, no. 5, pp. 1626 – 1636, 2004.

[20] J. Du, Y. Li, D. Gu, A. F. Molisch, and J. Zhang, "Estimation of performance loss due to delay in channel feedback in MIMO systems," *IEEE Vehicular Technology Conference*, vol. 60, no. 3, pp. 1619 – 1622, 2004.

[21] K. R. Dandekar, A. Arredondo, H. Ling, and G. Xu, "Modeling and prediction of the wireless vector channel encountered by smart antenna systems," *Microwave and Optical Technology Letters*, vol. 35, no. 4, pp. 281 – 283, 2002.